increasing level of theory the position of the energy minimum shifts from 180° (HF) to 145° (MP3), 140° (MP4SD), and 130° (MP4SDQ), and the energy relative to the linear configuration decreases by 0.28 (MP3), 0.54 (MP4SD), and 0.92 (MP4SDQ) kJ·mol^{-1}. These calculations thus confirm the ab initio results for the model compounds $HCSH_3$ and $FCSH_3$, in that higher levels of electron correlation increase the degree of bending, and definitely result in a bent equilibrium configuration of the C—C≡S skeleton in $CF_3C{\equiv}SF_3$, in agreement with the experimental data.

Comparison of Structure and Thermal Chemistry of Stoichiometric and Catalytic Alkoxy-Substituted Molybdenum Heteropolyanions: ^{13}C CP-MAS NMR Spectrum of a Chemisorbed Reaction Intermediate

W. E. Farneth,* R. H. Staley, P. J. Domaille, and R. D. Farlee

Contribution from E. I. du Pont de Nemours and Co., Central Research and Development Department, Experimental Station, Wilmington, Delaware 19898. *Received October 27, 1986*

Abstract: This paper reports the spectral and chemical properties of methanol chemisorbed on $K_{3-x}H_xPMo_{12}O_{40}$. The heterogeneous gas/solid reaction was investigated by a variety of techniques including the following: vacuum gravimetric measurements, temperature-programmed desorption, infrared spectroscopy, solid-state ^{13}C CP-MAS NMR, and comparison with stoichiometric model compounds. It is demonstrated that residual proton content in the heteropolyanion (HPA) salt plays an important role in the generation of reactive, chemisorbed intermediates. A methoxy group that occupies a bridging site in the HPA lattice is shown to be a key intermediate on the pathway to both dehydration and oxidation products. The structure of the methoxy intermediate is confirmed by spectral comparison with an identical, methylated Keggin anion salt of known structure.

Heteropolyacids and their salts occupy an interesting intermediate structural position between solid state metal oxides and small mono- or bimetallic coordination compounds. They are discrete molecular clusters containing 6, 12, or larger numbers of metal atoms linked through oxide bridges.[1] Because they are discrete molecular systems they are easier to characterize and rationally modify than the surfaces of metal oxide solids. Their chemistry and spectroscopy therefore offer great promise as a model for heterogeneous metal oxide catalyst systems. In addition, many heteropolyanion systems are interesting as catalytic materials in their own right.[2] The confluence of these two incentives has led to a growing effort to understand the electronic structure, spectra, and chemistry of these compounds, particularly the best known class of $XM_{12}O_{40}$ compounds having the so-called Keggin structure. In this paper we report the spectral and chemical properties of methanol chemisorbed on $K_{3-x}H_xPMo_{12}O_{40}$ and an alkylated analogue of this heteropolyanion, $Cs_2(OCH_3)PMo_{12}O_{39}$. We demonstrate that (1) residual proton content in the heteropolyanion salt plays an important role in the mechanism of alcohol oxidation over these materials, (2) a methoxy intermediate is formed on the heteropolyanion surface during chemisorption, (3) the surface methoxy formed by dissociative chemisorption of methanol is spectroscopically and chemically similar to that formed by direct alkylation in solution and, therefore, probably occupies a bridging site in the HPA skeleton, and (4) this intermediate can be involved in a redox cycle that leads to "O" atom loss from the HPA. The adsorbed methoxy described in this paper is one of only a handful of chemisorbed heterogeneous reaction intermediates that has been directly observed by solid-state NMR.

Experimental Section

$K_{3-x}H_xPMo_{12}O_{40}$ was prepared by precipitation from a solution of $H_3PMo_{12}O_{40}{\cdot}nH_2O$ and K_2CO_3 in H_2O. The components were added in a molar ratio of 2/3 at $n = 30$.[4] The precipitate was filtered, washed with distilled water, and dried. The material is a bright yellow, polycrystalline powder. Electron microscopy shows it to consist of roughly spherical particles of 0.2-1.0-μm diameters, with prominent surface irregularities. Although literature would suggest that this is a preparation procedure for $K_3PMo_{12}O_{40}$, the elemental analysis data, and especially the chemistry and spectroscopy (vide infra), make it clear that $K_{3-x}H_xPMo_{12}O_{40}$ is a better representation of the molecular formula for this material. Elemental analyses were obtained from Mikroanalytisches Labor Pascher, Bonn, West Germany. Calcd for $K_3PMo_{12}O_{40}{\cdot}5H_2O$: K, 5.78; P, 1.53; Mo, 56.73; O, 35.48; H, 0.49. Found: K, 4.85; P, 1.60; Mo, 58.30; O, 34.60; H, 0.48. The BET surface area is ~60 m^2/g, in reasonable accord with previous reports, and indicative of significant porosity in these particles. Goodenough et al. have recently shown that solid-state ^{31}P NMR and X-ray diffraction are both capable of detecting the presence of a discrete $H_3PMo_{12}O_{40}$ phase in $K_3PMo_{12}O_{40}{\cdot}5H_2O$ samples.[5] The ^{31}P solid state NMR (Nicolet NT-360, operating at 146.095 MHz with magic-angle spinning) of this sample is very clean. Only a single sharp peak at −3.9 ppm (fwhm = 0.5 ppm) relative to external 85% orthophosphoric acid is observed. Similarly, the X-ray powder pattern (2θ = 2-60°, Philips APD-3600) is identical with that previously reported for $K_3PMo_{12}O_{40}$ and shows no additional features that could be associated with a discrete H_3 phase.[5]

^{13}C magic-angle spinning (MAS) spectra were obtained on both a General Electric S-100 spectrometer (25.2 MHz) and a Bruker CXP-300 spectrometer (75.5 MHz). Dry nitrogen gas was used to drive MAS at rates of 2.5 kHz (S-100) to 4 kHz (CXP-300). The magic angle was set by minimizing the line width of the side bands of the Br-79 satellite transitions in KBr.[6] The Hartmann-Hahn matching condition for

(1) Pope, M. T. *Heteropoly and Isopoly Oxometalates*; Springer-Verlag: Berlin, 1983.

(2) (a) Misono, M. In *Catalysis by Acids and Bases*; Imelik, B. et al. Eds.; Elsevier: Amsterdam, 1985; p 147. (b) Renneke, R.; Hill, C. L. *J. Am. Chem. Soc.* **1986**, *108*, 3528.

(3) See Finke et al. (Finke, R. G.; Rapko, B.; Saxton, R. J.; Domaille, P. J. *J. Am. Chem. Soc.* **1986**, *108*, 2947) for a thorough discussion of the problems in preparation and characterization of these types of compounds.

(4) Tsigdinos, G. A. *Ind. Eng. Chem. Prod. Res. Dev.* **1974**, *13*, 267. n = 30 was established from TGA data.

(5) Black, J. B.; Clayden, N. J.; Gai, P. L.; Scott, J. D.; Serwicka, E.; Goodenough, J. B. *J. Catal.*, in press.

(6) Frye, J. S.; Maciel, G. E. *J. Magn. Reson.* **1982**, *48*, 125.

0002-7863/87/1509-4018$01.50/0

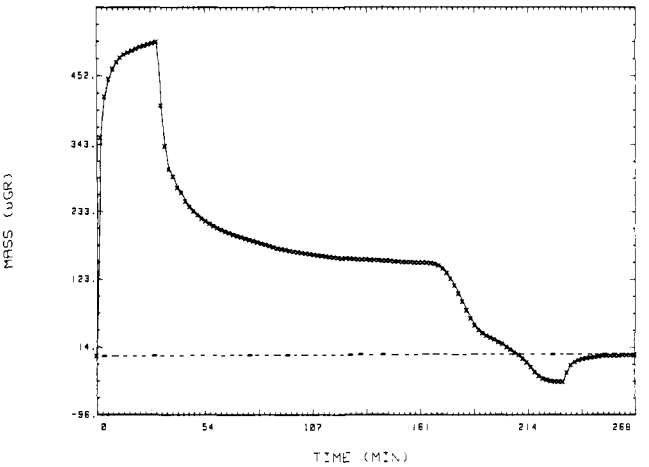

Figure 1. Mass changes observed during the methanol adsorption/evacuation/heating/reoxidation cycle on 25.530 mg of $K_{3-x}H_xPMo_{12}O_{40}$ (methanol exposure 10 Torr, 30 min). The dashed line represents initial sample mass.

cross-polarization (CP) was calibrated with adamantane, and both CP (2–5 ms) and decoupling (40 ms) were performed at the same proton decoupling amplitude ($\gamma(H_2)/2\pi$ = 50 kHz (S-100) or 68 kHz (CXP-300)). Between 1 000 and 15 000 scans were acquired with a 4-s recycle delay. Chemical shifts are reported relative to $(CH_3)_4Si$ with use of an external sample of adamantane as reference. Only small spinning side bands were observed in the spectra reported here, indicative of small chemical shift anisotropy, as would be expected for methoxy carbons.

The preparation and X-ray structural characterization of $((C_6H_{13})_4N)_2(OCH_3)PMo_{12}O_{39}$ has been previously reported.[7] The microbalance/temperature-programmed reaction apparatus has also been previously described.[8] All dosing gases were spectral grade and purified by vacuum transfer prior to use. IR spectra were taken in transmission mode using self-supporting pellets of $K_3PMo_{12}O_{40}$ powder. The pellets are mounted in a cylindrical open-ended quartz oven inside a metal vacuum system in the sample compartment of a Nicolet 700 FTIR. All spectra are shown as difference spectra between an experimental and reference condition as described in the figure captions.

Results

The chemisorption of methanol on $K_{3-x}H_xPMo_{12}O_{40}$ in a high-vacuum environment was followed gravimetrically. Approximately 20 mg of the bright yellow powder was placed in the sample pan of a Cahn-RG microbalance enclosed in a vacuum chamber. The system was pumped down to a base pressure of 10^{-8} Torr with use of a combination of sorption and cryo pumping. During this time, a loss of 4.1% of the sample mass occurred. Subsequent heating to 300 °C under vacuum produced an additional weight loss of 0.3%. Samples pretreated in this way were carried through adsorption, temperature-programmed desorption, and reoxidation cycles while changes in the sample mass were continuously monitored. The mass changes observed in a typical experiment involving exposure to 10 Torr of methanol for 30 min are shown in Figure 1.

The sequence begins with exposure to methanol vapor at some chosen combination of temperature, time, and pressure. Mass increases due to adsorption are observed (t = 0–30, Figure 1). Following the adsorption period, the system is pumped back to a base pressure of $<1 \times 10^{-7}$ Torr (t = 30–170, Figure 1), and the temperature is increased in a linear ramp from 25 to 300 °C. The sample mass falls as material desorbs (t = 170–230). The microbalance data appear to resolve two desorption events over this temperature range. The partial pressures of desorbing gases are followed by mass spectroscopy during this phase of the experiment. As shown in Figure 1, after the desorption period there has been a net weight loss of a few tenths of a percent. Exposure to O_2 (10 Torr/30 min) at 300 °C restores the sample mass to its original value (t = 230–260). The entire cycle has been

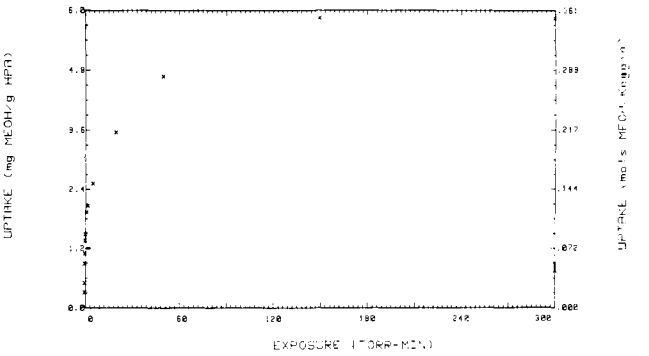

Figure 2. Chemisorption isotherm for methanol on $K_{3-x}H_xPMo_{12}O_{40}$ at 25 °C. Molar uptake is calculated assuming methanol adsorbs intact under these conditions.

repeated as many as six times in succession on a single sample without significant changes in behavior. The redox chemistry is accompanied by reversible color changes. The sample, which is initially bright yellow, acquires a greenish tinge following the chemisorption/temperature-programmed desorption sequence. Reoxidation restores the original yellow color. However, the sample is not particularly resilient. Heating to 400 °C under vacuum destroys the capacity of the powder to adsorb methanol appreciably and leads to a noticeable darkening of the sample. Carrying out the reoxidation at 325 °C rather than 300 °C leads to a marked loss of activity within three reduction–reoxidation cycles.

As shown in Figure 1, the uptake of methanol on $K_{3-x}H_xPMo_{12}O_{40}$ is substantial and occurs rapidly on exposure. At 10 Torr of methanol, total uptake saturates at ~1.5 methanol molecules per Keggin unit. The bulk of this adsorbate pumps away at room temperature, leaving a strongly bound, chemisorbed residual. The chemisorption is manifested in the increased mass at t = 161 min in Figure 1. The extent of chemisorption is a function of exposure. Figure 2 shows the chemisorption in g of methanol/g of solid, for various initial methanol exposures following pump-down to a background of 1×10^{-7} Torr. These values do not represent completely stable mass changes. Further pumping will continue to decrease the measured uptake, although beyond 1×10^{-7} Torr, by only minor amounts. On the right-hand ordinate, the mass changes are represented as the number of methanol molecules adsorbed per Keggin unit in the bulk sample. This calculation assumes that methanol adsorbs intact under these conditions. Spectral data (vide infra) support this assumption.

The evolution of gases from the surface during the temperature ramp (t = 170–230; T = 25–325 °C) is followed along with the mass changes. The two desorption events evident in the gravimetric data are shown by mass spectrometry to involve quite different chemistry. In the low-temperature peak, ~140 °C, H_2O and CH_3OH predominate. A smaller amount of CH_3OCH_3 is also indicated. In the higher temperature range, >250 °C, CH_2O, CO, and H_2O are the principal species desorbing. The desorption profiles of the most important evolved gases are represented in Figure 3. These profiles are generated either by directly plotting the intensity changes in one m/e value that is unique to a single species, for example, m/e 32 is used to monitor methanol, or by spectral subtraction of contributions to a given m/e intensity due to fragmentation of a second species, for example, m/e 30 is used to monitor formaldehyde after appropriate (small) corrections for fragmentation of methanol. For all of the species produced in this relatively simple system, these methods are sufficient to generate species-specific partial-pressure profiles. Mass spectral intensities have not been corrected for sensitivity differences and therefore do not represent absolute partial pressures. It is the shape of the profiles and the congruence or noncongruence of the profiles that we have found most informative.

The progress of the heterogeneous chemistry of methanol over $K_{3-x}H_xPMo_{12}O_{40}$ has also been followed spectroscopically by using both transmission IR and solid-state ^{13}C NMR. Samples for ^{13}C NMR were prepared under vacuum under conditions identical

(7) Knoth, W.; Harlow, R. L. *J. Am. Chem. Soc.* **1981**, *103*, 4265.
(8) Farneth, W. E.; Ohuchi, F.; Staley, R. H.; Chowdhry, U.; Sleight, A. W. *J. Phys. Chem.* **1985**, *89*, 2493.

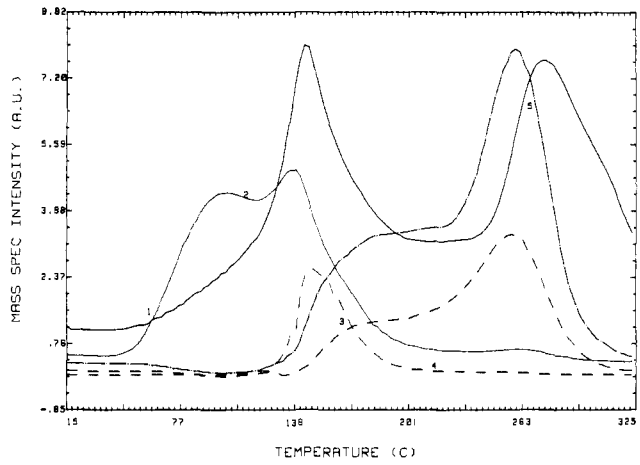

Figure 3. Temperature-programmed reaction profiles from $K_{3-x}H_xPMo_{12}O_{40}$ after a 300 Torr·min methanol exposure at 25 °C (curve 1 = water, curve 2 = methanol, curve 3 = formaldehyde, curve 4 = dimethyl ether, curve 5 = carbon monoxide). The mass spectral intensities are not corrected for detector sensitivity and therefore do not represent absolute partial pressures.

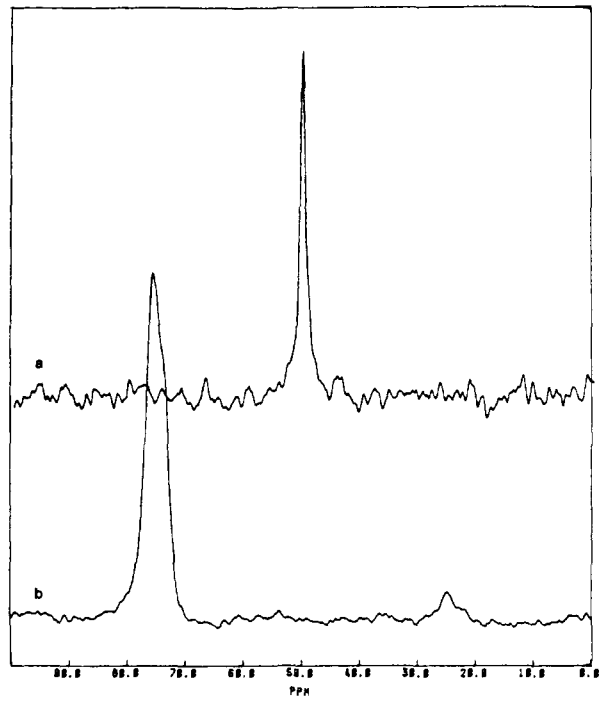

Figure 4. ^{13}C CP-MAS NMR spectra of species present on $K_{3-x}H_xPMo_{12}O_{40}$ after a 300 Torr min methanol dose and (a) heating to 50 °C under vacuum (b) heating to 150 °C under vacuum.

with those of the TPD experiments. Briefly, ~500-mg samples were pretreated by heating in O_2 at 300 °C, evacuated to $<10^{-7}$ Torr, and dosed with 90% $^{13}CH_3OH$ at 23 °C. After dosing, physisorbed material was pumped away. To generate Figure 4a, the solid-adsorbate system was sealed and removed from the vacuum. The sealed tube was opened in a glovebox under N_2 atmosphere, transferred to a sapphire rotor, capped, and inserted in the NMR probe. To generate Figure 4b, the sample was heated to 150 °C under vacuum before sealing and removing. Spectra a and b in Figure 4 therefore correspond to points at t = 161 and 186 min in Figure 1, respectively. ^{13}C CP-MAS NMR spectra were typically run at 75.5 MHz. Shifts are reported relative to external tetramethylsilane. Spectrum a in Figure 4 is dominated by a sharp transition at 51 ppm, and no other features are observed. The ^{13}C isotropic chemical shift of liquid methanol is 49.6 ppm. Thus, most of the methanol held on the polycrystalline powdered sample at room temperature is only slightly perturbed from free alcohol. However, heating to 150 °C results in a

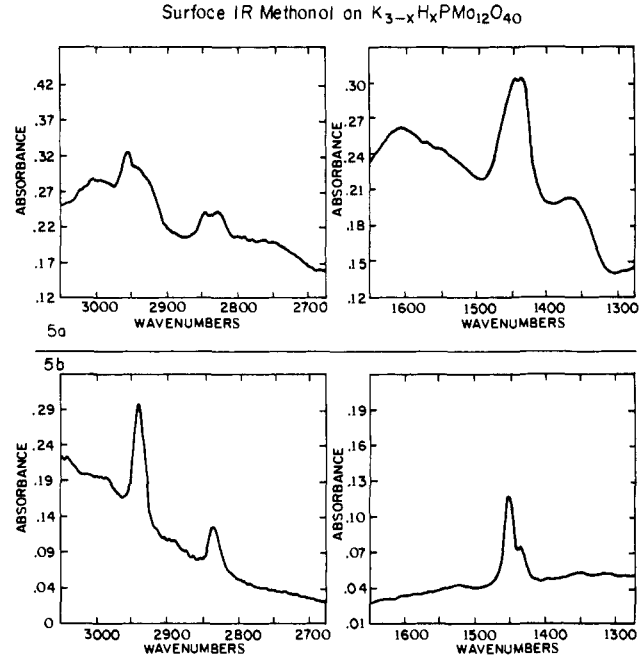

Figure 5. Transmission IR spectra of surface species present on $K_{3-x}H_xPMo_{12}O_{40}$ pellet after exposure to 10 Torr of methanol for 10 min and (a) heating to 50 °C or (b) heating to 150 °C.

Table I

adsorbate bands (cm^{-1})[a]			
50 °C	150 °C	assignment	species[b]
3400		O–H str	MeOH, –OH
	3320	O–H str	–OH
2955 (sh)		CH_3 as. str	MeOH
	2940	CH_3 as. str	–OMe (2935)
2845		CH_3 s str	MeOH
	2835	CH_3 s str	–OMe (2830)
2825		CH_3 s str	MeOH
	1450 (sh)	CH_3 def	–OMe (1450)
1445		CH_3 def	MeOH
1435		CH_3 def	MeOH
1370		C–OH bend	MeOH

[a] sh indicates the presence of a prominent shoulder at lower frequency. [b] Numbers in parentheses are observed frequencies for methoxy groups on the surface of MoO_3 (ref 21).

dramatic change in the NMR spectrum shown in Figure 4b. The spectrum appears to consist of a major species with a chemical shift of 75 ppm, well downfield from normal methanol. The barely resolved shoulder on the upfield side of this peak may imply the presence of a minority species as well. These shifts are within the range expected for metal–methoxy species.[9]

This picture of the surface chemistry is reinforced by the infrared spectral data shown in Figure 5. These are transmission spectra of pressed pellets of heteropolyanion salt exposed under vacuum to the same treatment as the NMR samples, spectra a and b in Figure 4. Upon exposure to methanol at 50 °C, peaks shown in Figure 5a appear in the C–H stretching region (2800–3050 cm^{-1}), in the bending region (1300–1600 cm^{-1}), and in the O–H stretching region (3200–3650 cm^{-1}) (not shown). Specific assignments are listed in Table I. In general, the peak positions are consistent with intact adsorbed methanol, although peaks in both the stretching and bending regions are doubled and suggest that there are probably two different methanol species adsorbed. After the sample is heated to 150 °C the spectrum shown in Figure 5b is obtained. Single peaks are now observed in C–H symmetric and antisymmetric stretching. In the bending region, the peak at 1450 cm^{-1} has narrowed and sharpened, al-

(9) (a) Liang, S. H. C.; Gay, I. D. *Langmuir* **1985**, *1*, 593 and references therein. (b) Vide infra.

though it still appears to have a shoulder on the low-frequency side. These frequencies are in excellent agreement with expected positions for adsorbed Mo–methoxy species (Table I).[10]

The Keggin anion structure could support either terminal or bridging methoxy ligands. In fact, in general, in the metal oxide chemistry of alcohols, terminal and bridging oxygen atoms are available, and distinguishing between them as sites for chemisorption is an important and difficult problem.[11] In this case, we are convinced that the adsorbed methoxy occupies a bridging coordination site. This conclusion is based on a comparison of the spectral properties of the adsorbate with a stoichiometric model compound whose structure has been proven by X-ray crystallography. Knoth has shown that heteropolyanion systems can be alkylated in solution through the reaction of the organic-soluble salts with trialkyloxonium tetrafluoroborate.[7] Using this method, he has prepared a variety of HPA derivatives including the methylated phosphomolybdic acid salt, $[(n\text{-}C_6H_{13})_4N]_2OCH_3PMo_{12}O_{39}$. This crystalline solid shows a ^{13}C CP MAS spectrum with a single carbon resonance at 74.7 ppm assigned to the methoxy carbon atom.[12] This chemical shift is essentially identical with that of the adsorbed methoxy shown in Figure 4b. Molybdenum methoxides in other model compounds of related structure include the following: $Mo(OCH_3)_6$, 64 ppm; $Mo_2O_5(OCH_3)_2$, 72 ppm; and $Na_4[Mo_8O_{24}(OCH_3)_4]\cdot 8H_2O$, a compound known to contain both bridging and terminal methoxy ligands, 72 and 69 ppm. We take the excellent agreement between the ^{13}C shifts in the adsorbate and the stoichiometric analogue to be strong evidence that they have the same structure. This conclusion is reinforced by IR data on the cesium salt of the alkylated HPA, which shows C–H bending and stretching bands at 2950, 2850, and 1440 cm^{-1}, in good agreement with the adsorbate IR data. The crystal structure of the model compound, $[(n\text{-}C_6H_{13})_4N]_2OCH_3PMo_{12}O_{39}$, has been reported, and the methoxy has been shown to occupy a bridging site between two molybdenums in a single Mo_3 triad.[7]

There are additional changes in the spectral characteristics of the adsorbate that occur upon further heating above 200 °C. For example, the C–H stretching region of the IR spectrum is reduced in intensity, but it shows no new peaks. However, the region between 1200 and 1600 cm^{-1} grows considerably more complex. The structure of the adsorbate(s) responsible for these spectral features is not known at this time.

Discussion

Heteropolyanions have been investigated both as heterogeneous acid catalysts[13] and as catalysts for oxidation reactions.[14,15] It has been demonstrated, for example, that methanol can be converted to hydrocarbon mixtures with varying efficiencies over a number of heteropolyacids and/or HPA salts and that methacrolein can be efficiently oxidized to methacrylic acid. For the methanol-to-hydrocarbons chemistry, a consensus seems to have emerged that the reaction sequence is initiated by interaction of alcohol molecules with Bronsted acid sites on the HPA catalysts.[16] For some types of oxidation chemistry, Bronsted acidity has also been suggested to be important in generating surface intermediates that can decompose by reductive elimination from the catalyst.[17] We believe that Bronsted acid sites associated with residual proton content in the HPA salt also play an important role in the chemistry that we have examined.

Spectroscopic evidence for residual protons in the HPA salt comes from both IR and NMR. Significant proton signals could be observed by solid-state ^1H NMR. By comparing the amplitude of the free induction decay of the sample with that of a reference water sample, an estimate of the number of protons in the sample could be obtained. After evacuation at room temperature approximately 0.75 H per Keggin unit were counted. After a standard pretreatment sequence (heat to 300 °C in O_2, cool in vaccum) on the order of 0.15 protons per Keggin anion were observed. IR studies also indicate the existence of protons in the dehydrated HPA salt. The transmission IR spectrum of a sample evacuated to 1×10^{-7} Torr at 25 °C shows a large, broad feature in the hydroxyl stretching region, with maximum absorbance at ~3300 cm^{-1}. This feature diminishes in intensity as the sample is heated under vacuum, although it is still apparent after a standard pretreatment sequence. However, the most compelling evidence for Brønsted acidity in these samples comes from pyridine titrations on the pretreated catalyst. Figure 6 shows the transmission IR observed after the sequence: heat to 300 °C in O_2, cool to 150 °C, evacuate, expose to pyridine at 100 mTorr for 5 min, evacuate. The features shown in Figure 6 are in excellent agreement both in peak position and in relative intensities with previous assignments for chemisorbed pyridinium ions.[18]

Some indication that significant numbers of protons have been retained in this powder is given by the elemental analysis. The K/Mo ratio observed was 0.083, whereas the expected value for $K_3PMo_{12}O_{40}$ is 0.102. In contrast to this, a sample of the cesium salt of $PMo_{12}O_{40}$ prepared in an identical fashion gave observed and calculated Cs/Mo ratios of 0.355 and 0.346, respectively. Significantly, the cesium salt showed very little chemisorption of methanol, in spite of a 3 times larger surface area.

In contrast to these clear indications of residual proton content in this HPA sample, neither X-ray powder spectra nor ^{31}P NMR show any evidence for a discrete $H_3PMo_{12}O_{40}$ phase. Both of these techniques give results in excellent agreement with previously reported $K_3PMo_{12}O_{40}$ spectra. We are inclined to think of the protons as an epitaxial layer present on the surface of the K_3 crystallites. This suggestion has been previously advanced by Goodenough et al., who also pointed out the plausibility of a proton-containing surface layer when the insoluble K_3 salt precipitates from aqueous solution.[5]

The Brønsted acidity of the surface plays a key role in the methanol chemistry that $K_{3-x}H_xPMo_{12}O_{40}$ promotes. Moffat has presented strong evidence for the following mechanism for the conversion of methanol over the corresponding heteropolyacid, $H_3PMo_{12}O_{40}$, at low temperatures.[19]

$$CH_3OH + H^+\cdots O_{ku} \xrightarrow{25\ ^\circ C} CH_3{}^+OH_2\cdots O_{ku} \quad (1)$$

$$CH_3{}^+OH_2\cdots O_{ku} \xrightarrow{50\text{–}150\ ^\circ C} CH_3{}^+\cdots O_{ku} + H_2O \quad (2)$$

$$CH_3{}^+\cdots O_{ku} + CH_3OH \xrightarrow{>25\ ^\circ C} CH_3OCH_3 + H^+\cdots O_{ku} \quad (3)$$

(ku represents a species bound in the Keggin unit framework)

Our results on the potassium salt under vacuum can be understood within the same framework, where H^+ represents residual surface Brønsted sites. Under the conditions of these experiments, the methoxy intermediate can participate in both HPA-initiated redox chemistry and the dehydration reaction shown in step 3 above. Therefore we may extend the mechanistic scheme as follows:

$$CH_3{}^+\cdots O_{ku} + O_{ku} \xrightarrow{>200\ ^\circ C} CH_2O + H^+\cdots O_{ku} \quad (4)$$

$$CH_2O + O_{ku} \xrightarrow{>200\ ^\circ C} CO + H_2O \quad (5)$$

We will use this mechanistic scheme as a framework for analyzing our observations on the chemistry of this system in the discussion below.

(10) Groff, R. P. *J. Catal.* **1984**, *86*, 215.
(11) Goodenough, J. B. In *Proceedings of the Climax 4th International Conference on Chemistry and Uses of Molybdenum*, Barry, H. F., Mitchell, P. C. H., Eds.; Climax Molybdenum Co.; Ann Arbor, 1982.
(12) ^{13}C signals which can be assigned to the individual carbon resonances in the *n*-hexylammonium cation are also observed at higher magnetic field.
(13) McMonagle, J. B.; Moffat, J. B. *J. Catal.* **1985**, *91*, 132.
(14) Akimoto, M.; Ikeda, H.; Okabe, A.; Echigoya, E. *J. Catal.* **1984**, *89*, 196.
(15) Mizuno, N.; Watanabe, T.; Misono, M. *J. Phys. Chem.* **1985**, *89*, 80.
(16) Highfield, J. G.; Moffat, J. B. *J. Catal.* **1986**, *98*, 245.
(17) Ai, M. *J. Catal.* **1984**, *85*, 324.
(18) (a) Parry, E. P. *J. Catal.* **1963**, *2*, 37. (b) Misono, M.; Mizuno, N.; Katamura, K.; Kasai, A.; Konishi, Y.; Sakata, K.; Okuhara, T.; Yoneda, Y. *Bull. Chem. Soc. Jpn.* **1982**, *55*, 400.
(19) Highfield, J. G.; Moffat, J. B. *J. Catal.* **1985**, *95*, 108.

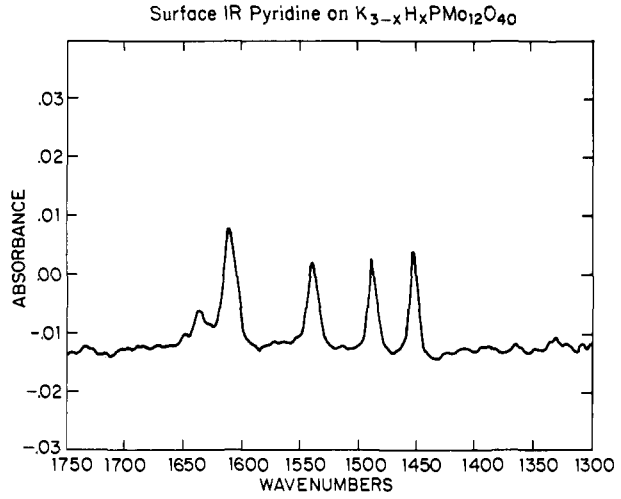

Figure 6. Transmission IR spectra of surface species present on $K_{3-x}H_xPMo_{12}O_{40}$ pellet exposed to 100 mTorr of pyridine at 150 °C for 10 min.

Step 1 indicates a specific interaction of methanol molecules with acidic heteropolyanion sites, creating an oxonium ion/Keggin anion pair. The spectral data imply such a specific interaction, but they do not offer firm evidence for complete proton transfer to give the oxonium ion structure. The IR spectra of the O–H region indicate that there are H-bonding interactions involved in chemisorption, and the small downfield shift in the ^{13}C NMR relative to pure methanol is consistent with the chemisorbed structure. However, no IR bands at frequencies suggested by Moffat for a $CH_3OH_2^+$ species on $H_3PW_{12}O_{40}$ are obvious in our spectra.[19] The gravimetric data give a concentration of one adsorbed methanol per 2.5 Keggin units after a saturation dose at 25 °C. This exceeds the concentration of protons in the sample, which we have estimated by ^1H NMR to be <1 per 6 Keggin units. Therefore it appears that some nonspecifically bound methanol molecules are also retained on the catalyst. These "solvent" methanol molecules may be responsible for the low-temperature shoulder in the methanol desorption trace shown in Figure 3.

Steps 2 and 3 occur simultaneously in the low-temperature stage of the heating ramp, T = 25–150 °C. The chemistry is manifest in the desorption of H_2O, CH_3OCH_3, and CH_3OH and in the spectroscopic observation of a newly formed surface methoxy. We believe that the decomposition of the adsorbed alcohol, step 2, initiates the chemistry. The bridging methoxy ligand formed in this decomposition may then be trapped by evolving methanol to generate dimethyl ether. If the sample containing adsorbed methanol is heated to 150 °C and then cooled to 25 °C and reheated, no desorption is observed below 150 °C, and the high-temperature desorption spectrum is essentially unchanged. The complementary spectroscopy also indicates that the desorption peaks below 150 °C and above 150 °C are effectively two independent decomposition events initiated from different adsorbed intermediates. The low-temperature peak involves intact adsorbed alcohol as a reactant and C–O bond cleavage, the higher temperature peak, a surface methoxy intermediate and C–H bond cleavage. Evidence that this is the right sequence of events comes from the thermal decomposition of the stoichiometric model system, $(OCH_3)Cs_2PMo_{12}O_{39}$. The product distribution observed when this compound is heated under vacuum is complex. It includes both oxidation products and hydrocarbons. However, no products are evolved at temperatures below 200 °C. Therefore, when methanol is not present in the vapor, the surface methoxy groups appear to be stable toward desorption, until the temperature range associated with the second peak in Figure 3.

At t = 186 min ($T \cong$ 175 °C) in Figure 1, that is between the events associated with the formation of the methoxy and its decomposition, the residual mass is approximately 0.030 mg of adsorbate. If we assume that this mass represents only chemisorption of formal CH_3^+ units, as the spectroscopy suggests, then there is 1 CH_3^+ per 7 Keggin units present on the surface at this point. The stoichiometry of steps 1 and 2 requires that 1 formal CH_3^+ unit will be formed for each proton involved in oxonium ion formation during the initial methanol dose. The number of CH_3^+ retained at 200 °C will be reduced, however, to the extent that they are scavenged by step 3. The measured proton count of 0.15 per Keggin anion present after pretreatment and before methanol exposure would suggest, as an upper limit, a concentration of 1 CH_3^+ per 6.66 Keggin units. This estimate is in excellent agreement with the mass data described above.

Steps 1–3 alone do not rationalize the appearance of methanol as an important contributor to the low-temperature desorption. The gravimetric data indicate that after dosing and pumpdown there is a population of adsorbed alcohol molecules that is not directly associated with acid sites on the Keggin anions. This population may be responsible for the low-temperature shoulder on the methanol peak. However, the double-humped methanol profile implies that there is another source as well. It is possible that this second source is simply desorption of methanol from the bound oxonium ion with reprotonation of the HPA. Another possibility, however, is that the intermediate involved in ether formation, $CH_3O(H)CH_3^+$, may have some lifetime on the surface and decompose not by proton transfer as represented by step 3 but by methyl transfer back to the Keggin framework, as the temperature is raised, reforming the reactants, CH_3OH and $CH_3^+\cdots O_{ku}$.

Step 4 represents the decomposition of the surface methoxy by proton transfer to an oxide ligand. This is the rate-limiting step for alcohol oxidation on α-MoO_3.[8] The methoxy decomposition reaction on the Keggin ion and α-MoO_3 systems occur at similar temperatures (T_{max}(formaldehyde) = 265 °C on $K_3PMo_{12}O_{40}$; T_{max}(formaldehyde) = 210 °C on α-MoO_3). These T_{max} differences may imply something about the relative proton affinities of the proton-accepting sites on the two catalysts, but the interpretation of T_{max} data can be complicated by diffusion and mass transport effects, so more detailed interpretation is probably not justified. However, as with the methanol/α-MoO_3 system, there is a substantial isotope shift of the formaldehyde desorption peak from methanol/$K_3PMo_{12}O_{40}$. After dosing with methanol-d_4, the formaldehyde peak moves to higher temperatures by 15 °C. The high-temperature water peak associated with step 5 in the mechanism also shifts to higher temperature and appears predominantly as D_2O. In both cases, therefore, the decomposition transition state clearly involves significant C–H bond stretching and formaldehyde formation as a primary product. Dosing with methanol-d_3, and examining the hydroxyl region by IR, shows O–H stretching bands that are present below 150 °C are replaced by O–D stretching bands as C–D bonds begin to cleave above 150 °C.

Additional surface intermediates are involved in steps 4 and 5. CO is a much more important product in the heteropolyanion chemistry than in methanol reaction over α-MoO_3. This (these) additional intermediate may be involved in the further decay of the first-formed formaldehyde species. IR bands associated with this higher temperature surface species are sensitive to deuterium substitution at carbon in the adsorbed methanol. This suggests that they may involve C–H or O–H bending modes, but assignment of these spectra in the temperature range above 200 °C awaits further work.

Steps 4 and 5 suggest that this chemistry is of the Mars–van Krevelen type.[20] That is, the reduction of the catalyst is accompanied by oxygen atom loss from the matrix. This mechanism implies that the Keggin structure can tolerate some level of oxygen atom vacancy without loss of integrity. The microgravimetric data directly demonstrate this aspect of the mechanism. Figure 1 shows that the mass of the catalyst falls below its initial value after dosing and TPD and that this deficit can be completely restored by heating in oxygen. Since the entire chemisorption, temperature-programmed reaction, reoxidation cycle can be repeated a number of times without change, the Keggin structure is apparently preserved.

(20) Mars, P.; van Krevelen, D. W. *Chem. Eng. Sci. Suppl.* **1954**, *3*, 41.

Conclusions

In this work we have demonstrated that there are clear parallels between the heterogeneous and homogeneous chemistry of phosphomolybdate heteropolyanion systems. Surface intermediates that occur during a heterogeneous redox cycle in which methanol is oxidized have been isolated and compared to their stoichiometric counterparts by direct spectroscopic means. It has been established that the crucial intermediate is a methoxy group occupying a bridging site on the heteropolyanion framework. Because of the similarity of this chemistry to bulk metal oxide oxidations of alcohols, we expect further work on these systems to be a very fruitful strategy for clarifying the atomic scale picture of heterogeneous selective oxidation reactions.

Acknowledgment. The authors are grateful for the technical assistance of Willis Dolinger, Robert Carver, George Watunya, and James D. Simmons. Samples of the alkylated heteropolyanions were graciously provided by Walter Knoth. Solid-State ^1H NMR spectra were taken by A. J. Vega, to whom we are also grateful. W. E. Farneth would particularly like to thank J. B. Goodenough, E. M. Serwicka, and R. G. Finke for providing preprint copies of their manuscripts.

Cyanocarbon Acids: Direct Evidence That Their Ionization Is Not an Encounter-Controlled Process and Rationalization of the Unusual Solvent Isotope Effects

M. Hojatti, A. J. Kresge,* and W.-H. Wang

Contribution from the Department of Chemistry, University of Toronto, Toronto, Ontario M5S 1A1, Canada. *Received December 10, 1986*

Abstract: The rate of exchange of the acidic hydrogen of *tert*-butylmalononitrile was examined by using tritium as a tracer, and the process was found not to be inhibited by hydronium ions in dilute aqueous hydrochloric acid solutions. This rules out the Swain–Grunwald mechanism for this reaction under these conditions. The bromination of malononitrile was investigated under conditions where reprotonation of the dicyanomethyl carbanion and its reaction with bromine occur at comparable rates, and the bromination reaction was found to have a specific rate twice that for reprotonation. Reprotonation therefore cannot be a diffusion-controlled process, and malononitrile is not a "normal" acid. The unusually large solvent kinetic isotope effects found for these cyanocarbon acid ionization reactions are explained by postulating that the transferring hydrogen and its positive charge are becoming associated with a solvent cluster rather than with a single water molecule. The thermodynamic acidity constant of malononitrile was determined to be 11.41 in aqueous solution at 25 °C.

Cyanocarbons such as malononitrile (**1**) and *tert*-butylmalononitrile (**2**) constitute an important class of organic acids inasmuch as their proton-transfer reactions are almost "normal"

$$\underset{\mathbf{1}}{(CN)_2CH_2} \qquad \underset{\mathbf{2}}{(CN)_2CH(t\text{-}Bu)}$$

in the Eigen sense.[1,2] Normal acids and bases are species whose proton-transfer reactions are almost completely diffusion-controlled; only in a small region near $\Delta pK = 0$ is the proton-transfer step of the overall proton-transfer process even partly rate-determining, and when ΔpK deviates from zero by as little as 2–3 pK units, encounter of the reactants or separation of the products becomes fully rate-determining.[1,3,4] Most carbon acids are not "normal" in this sense: the proton-transfer steps of their acid–base reactions are wholly rate-determining over a wide range of ΔpK.

Although much of the acid–base chemistry of cyanocarbons is well-understood, some aspects remain puzzling. In particular, solvent isotope effects on the rate of ionization of these acids in aqueous solution are unexpectedly large. For example, isotope effects measured by monitoring the rate of loss of tritium from labeled substrates to water are $k_{H_2O}/k_{D_2O} = 3.7$ for malononitrile and $k_{H_2O}/k_{D_2O} = 3.5$ for *tert*-butylmalononitrile.[5] On the assumption that proton transfer is rate-determining but nearly complete at the transition states of these reactions, eq 1, these solvent isotope effects would be attributed to the conversion of

$$RT + L_2O \rightarrow [R\cdots\overset{\delta-}{T}\text{—}\overset{\delta+}{O}L_2]^{\ddagger} \rightarrow R^-\cdot TOL_2^+ \qquad (1)$$

two neutral hydrogen–oxygen bonds (L–O) to two positively charged ones (L–O^+), and they could be estimated by using fractionation factor theory[6] as $k_{H_2O}/k_{D_2O} = 1/l^2 = 2.1$. This difference between expected and observed values is made all the more remarkable by the fact that the isotope effect measured for detritiation of *tert*-butylmalononitrile when acetate ion rather than water is the proton acceptor, $k_{H_2O}/k_{D_2O} = 1.1$,[5] is not at all unusual.

These unexpectedly large isotope effects might be rationalized in terms of the Swain–Grunwald mechanism for diffusion-controlled isotope exchange reactions.[7] Although the evidence in-

(1) Eigen, M. *Angew. Chem., Int. Ed. Engl.* **1964**, *3*, 1–19.

(2) For a review of cyanocarbon acid–base behavior, see: Hibbert, F. In *Comprehensive Chemical Kinetics*, Vol. 8, Bamford, C. H., Tipper, C.F.H., Eds.; Elsevier: New York, 1977; Vol. 8, Chapt 2. See also Kreevoy et al. (Kreevoy, M. M.; Dolmar, J.; Langland, J. T. *Abstracts of Papers*, 166th National Meeting of the American Chemical Society; American Chemical Society: Washington, DC, 1973; PHYS 148) for the effect of viscosity on cyanocarbon ionization rate and Albery (Albery, W. J. In *Proton Transfer Reactions*; Caldin, E. F., Gold, V., Eds.; Chapman and Hall: London, 1975; pp 294–296) for a discussion of isotope effects.

(3) Bell, R. P. *The Proton in Chemistry*; Cornell University Press: Ithaca, NY, 1973; (a) p 130, (b) p 22.

(4) Bergman, N.-Å; Chiang, Y.; Kresge, A. J. *J. Am. Chem. Soc.* **1978**, *100*, 5954–5956. Cox, M. M.; Jencks, W. P. *J. M. Chem. Soc.* **1978**, *100*, 5956–5957; **1981**, *103*, 572–580. Fischer, H.; De Candis, F. X.; Ogden, S. D.; Jencks, W. P. *J. Am. Soc.* **1980**, *102*, 1340–1347.

(5) Hibbert, F.; Long, F. A. *J. Am. Chem. Soc.* **1971**, *93*, 2836–2840.

(6) Kresge, A. J. *Pure Appl. Chem.* **1965**, *8*, 243–258. Schowen, R. L. *Prog. Phys. Org. Chem.* **1972**, *9*, 275–332. Kresge, A. J.; More O'Ferrall, R. A.; Powell, M. F. In *Isotopes in Organic Chemistry*; Buncel, E., Lee, C. C., Eds.; Elsevier: New York, 1987; Vol. 7, Chapter 4.

(7) (a) Swain, C. G.; Labes, M. M. *J. Am. Chem. Soc.* **1957**, *79*, 1084–1088. Swain, C. G.; McKnight, J. T.; Kreiter, V. P. *J. Am. Chem. Soc.* **1957**, *79*, 1088–1093. Emerson, M. T.; Grunwald, E.; Kaplan, M. L.; Kromhout, R. A. *J. Am. Chem. Soc.* **1960**, *82*, 6307–6314. (b) Grunwald, E.; Ralph, E. K. *Acc. Chem. Res.* **1971**, *4*, 107–113. (c) Perrin, C. L.; Schiraldi, D. A.; Arrhenius, G. M. L. *J. Am. Chem. Soc.* **1982**, *104*, 196–201.

0002-7863/87/1509-4023$01.50/0